Estimation of strong ground motion in Southern Peninsular India by empirical Green's function method

K. Sivaram[1,*], Maheshreddy Gade[2], S. T. G. Raghukanth[3], Utpal Saikia[1,4] and Nagaraju Kanna[1]

[1]CSIR-National Geophysical Research Institute, Hyderabad 500 007, India
[2]School of Engineering, Indian Institute of Technology-Mandi, Kamand 175 005, India
[3]Department of Civil Engineering, Indian Institute of Technology-Madras, Chennai 600 036, India
[4]Present address: Indian Institute of Science Education and Research, Dr Homi Bhabha Road, Pashan, Pune 411 008, India

In the present study, strong motions are estimated at 17 stations in Southern Peninsular India (SPI) for the 7 February 1900 Coimbatore earthquake (M_w 6) using the empirical Green's function (EGF) method. The broadband recordings of three small earthquakes of M_L 3.5, 2.9 and 3.0 respectively, are taken as EGFs to simulate ground motion. The slip distribution of the main event is considered as a von Karman random field. The stress drops of the three small events estimated from finite fault stochastic seismological model lie between 130 and 140 bars. The peak ground acceleration (PGA) values, an ensemble of acceleration time histories and response spectra, are estimated at all the 17 stations using corresponding EGFs, and the mean response spectra are reported. Another estimate of PGA is also obtained using the stochastic seismological model. The estimated PGA values from the two methods are compared to check the consistency of the results. It is observed that the mean PGA values are within the bounds of the maximum and minimum PGA values obtained from the EGF method, while the differences at some stations can be attributed to the local site conditions.

The ground motions simulated in the present study can be used to perform nonlinear dynamic analysis for future and existing structures in the SPI region for any event of magnitude M_w 6.

Keywords: Empirical Green's function, ground motion, peak ground acceleration, response spectra, stochastic finite fault model.

EARTHQUAKES in the intraplate region of Southern Peninsular India (SPI) are found to be smaller in number and magnitude, compared to the seismically active and tectonic regions like the plate-boundary region of the Himalayas. However, a few devastating earthquakes have occurred in Peninsular India in the recent past, which pose a threat of such and larger earthquakes in the future. Unfortunately, the seismic recorded data are limited, based on which seismotectonic and earthquake engineering studies have been carried out in the past. SPI is one of the oldest and once known to be the seismically most stable land masses of the Indian plate. The earthquakes occurring unexpectedly in this stable continental region (SCR) have raised an alarm of the need to carry out seismic hazard analysis of the otherwise seismically ignored regions of SPI. Recently, Rajendran et al.[1] emphasized the seismic hazard by reassessing the earthquake hazard based on past and current seismicity in this region. For seismic hazard studies in this region, Iyengar and Raghukanth[2] developed the ground motion prediction equation (GMPE) based on accelerations simulated using the seismological model, and reported that attenuation of strong motion in Peninsular India is similar to that in other intraplate regions of the world. Raghukanth and Iyengar[3] proposed an attenuation relation for estimating 5% damped response spectra in Peninsular India using ground motions simulated from the seismological model. Engineers in India have been using design response spectra recommended by the code IS-1893 (ref. 4). However, one requires ground acceleration time histories to perform nonlinear dynamic analysis of important structures in this region. In the literature, analytical, numerical and empirical methods are available to simulate ground motions. Generally, accelerations are the primary input for seismic analysis of structures. It is well known that analytical and numerical methods are efficient in simulating accelerations controlled by low-frequency waves. On the other hand, empirical methods like empirical Green's function (EGF) and stochastic seismological methods are efficient in simulating accelerations which are controlled by high-frequency waves. As the earthquake data are limited in SPI, EGF technique using small earthquakes and stochastic seismological methods is used to simulate accelerations in the present study.

In this study, we examine the recent micro-earthquakes in SPI, and simulate the ground motion of the Coimbatore earthquake (1900, M 6), primarily using the method of EGF, first proposed by Hartzell[5], and modified by

*For correspondence. (e-mail: sivaramk@ngri.res.in)

Frankel[6]. To establish the consistency of the estimated ground motions from the EGF method, the stochastic finite fault model or seismological model is simultaneously applied on the dataset in SPI, following the method adopted in Raghukanth and Kavitha[7]. The obtained results from these two techniques are compared with National Disaster Management Authority (NDMA) report[8]. We also use existing peak ground acceleration (PGA) relationships with published damage reports. This would clear any disparity and provide a robust base for applications in seismic hazard and geotechnical analysis. We provide a review of the EGF method and the finite fault stochastic method in the subsequent sections. We first review the seismotectonic set-up of the study region, seismic data acquisition, followed by the methodology, and finally the summary and conclusion.

Seismotectonic set-up of the study region

The study region of SPI is geographically located between 8.0°–14.0°N and 75.0°–80.0°E. This region represents three major tectonic provinces: Dharwar craton, Eastern Ghat Mobile Belt and Southern Granulite Terrain (SGT). A detailed geological perspective of SPI is provided by Rai et al.[9]. In recent times, this stable region has produced several significant earthquakes. To account for the seismicity, the stress model of Rajendran et al.[10] provides a generalized tectonic framework in this region. Recently, Saikia et al.[11] have shown that the earthquakes in this region, especially those of SGT, near Idukki area, are likely of tectonic nature. They suggest that the geotectonic status pertaining to crustal structure and associated rift system of a majority of Peninsular India supports an intraplate tectonism leading to the occurrence of earthquakes. The 12 December 2000 Idukki earthquake (M 5.0) is a recent significant earthquake in this zone. Historically, the Coimbatore earthquake which occurred on 8 February 1900, M 6.0, intensity VII, is the largest known earthquake in the southern zone. This event was felt throughout the southern part of India, south of latitude 14°N, in which damages to houses were also reported.

Seismic data acquisition and preparation

Data acquisition was a part of the project: 'India Deep Earth Imaging Experiment' (INDEX), in which CSIR-National Geophysical Research Institute, Hyderabad, operated a network of 21 broadband seismographs during January 2011–March 2012 in the South Indian states of Tamil Nadu and Kerala to map the seismic pattern and image the deep structure of the region. These seismic stations are equipped with broadband 24-bit REFTEK data requisition system (RT 130/01 data recorder/digitizer), coupled with CMG3T broadband seismometers (GURALP-make) and GPS (global positioning system). In all the

seismic stations, the data recorders are operated with two 4-GB swappable flash cards, and record in continuous mode at 50 samples/sec. An external GPS allows synchronization of the internal clock of the REFTEK recorder/digitizer, and provides a time stamp with higher accuracy. All the equipment are powered by solar panels through a charge control unit and two 12 V sealed maintenance-free (SMF) batteries, which continuously provide the driving supply for the seismographs. The data are visually examined on the continuous waveforms using the REFTEK utility software, RTVIEW, and converted to SAC (Seismic Analysis Code) with instrument response and baseline corrections. For this work, the velocity waveforms were converted to accelerograms for all the stations. For the simulation of ground motion for the main Coimbatore earthquake, 17 out of the 21 stations were selected which had recorded the events with good signal-to-noise ratio, and clear phases for three small events (EGFs). Figure 1 shows the geological map of SPI, along with locations of the broadband recording stations, the three small events (EGF) shown as red stars (overlapped), the Coimbatore earthquake depicted as a larger
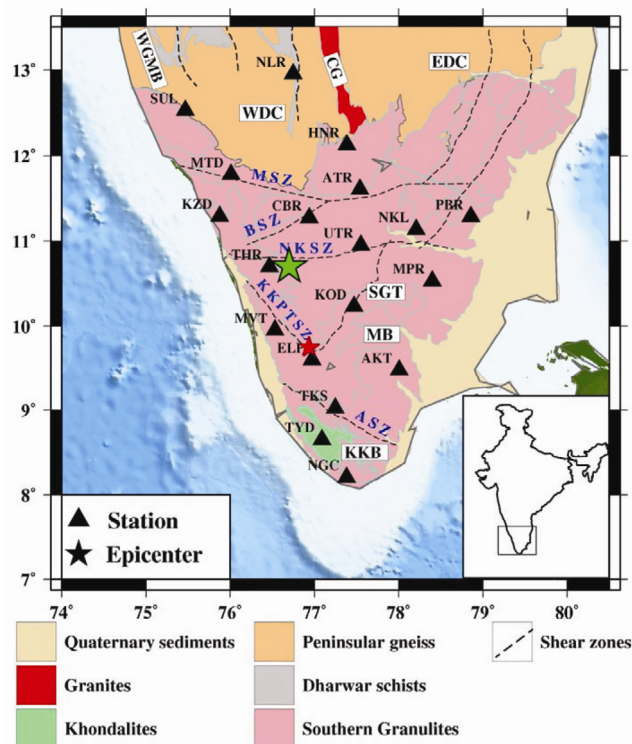
Figure 1. Seismic broadband recording stations (shown in black triangles and three-letter codes), operated by CSIR-National Geophysical Research Institute from 2009 to 2012 in the Southern Peninsular India (SPI). The epicentres of the three small events (empirical Green's functions, EGF) are shown as red stars (overlapped) and the main Coimbatore earthquake is shown as a larger green star. The map shows major geological terrains: EDC, Eastern Dharwar Craton; WDC, Western Dharwar Craton; SGT, Southern Granulite Terrain; CG, Closepet Granite; BSZ, Bhavani Shear Zone; NKSZ, Noyil Kaveri Shear Zone; GSZ, Gangavalli Shear Zone; ASZ, Achankovil Shear Zone; KKPTSZ, Karur Kambam Painavu Trichur Shear Zone.

Table 1. Details of origin time, magnitude and hypocentral parameters of the small events (empirical Green's function)

Date	UTC	Magnitude (M_L)	Epicentre		Focal depth (km)	Stress drop (bars)
			Latitude	Longitude		
26 July 2011	07:39:16.02	3.6	9.7533	76.9408	9.7	130
26 July 2011	08:45:55.52	2.9	9.7405	76.9447	9.9	132
18 November 2011	00:15:38.58	3.0	9.7543	76.9277	9.8	140

Table 2. Location details of broadband recording stations

Station	Latitude (°N)	Longitude (°E)	Epicentral distance (km)
Tharur (THR)	10.70	76.47	31.09
Uthiyur (UTR)	10.95	77.55	90.18
Muvazhipazla (MVT)	9.95	76.53	92.15
Kodaikanal (KOD)	10.23	77.47	97.62
Kuzikode (KZD)	11.29	75.87	113.35
Anthiyur (ATR)	11.60	77.54	127.99
Elappara (ELP)	9.60	76.97	130.12
Mannanthavaadi (MTD)	11.78	76.01	140.19
Hannur (HNR)	12.13	77.39	168.63
Mannaprai (MPR)	10.53	78.4	181.91
Aruppukkottai (AKT)	9.48	78.01	197.21
Tenkasi (TKS)	9.02	77.25	199.98
Theviyod (TYD)	8.65	77.09	236.45
Perambalur (PBR)	11.29	78.86	238.20
Sulaya (SUL)	12.53	75.47	242.34
Nelligere (NLR)	12.95	76.75	244.63
Nagercoil (NGC)	8.20	77.38	291.79

green star, in the background of the different geological boundaries. Details of the three EGFs are shown in Table 1 and location details of the 17 stations in Table 2 respectively. The focal mechanisms of the closely located small events considered here, as reported in Saikia et al.[11] were observed to have similar strike and dip angles with an average value of 322° for strike and 67° for dip respectively, in comparison to the main Coimbatore event, taken as 309° and 56° respectively[12].

Methodology of empirical Green's function

The first step in estimating ground motion for a given earthquake and specific station is to compute the Green's function which is defined as the response of the medium to unit impulsive force (double couple) in space and time. Due to computational difficulties and lack of lateral variation of material properties, the deterministic method based on plane-layered crustal models cannot capture high-frequency ground motions. If recordings of small events whose epicentres are located near the expected large earthquake are available, these can be treated as Green's functions. This technique of simulating ground motion using the small-magnitude records is known as EGF technique, originally proposed by Hartzell[5]. In the

present study, EGF method proposed by Frankel[6] is used to simulate ground motions for an M_w 6 damaging earthquake in SPI.

In the EGF approach, the rupture plane of the main shock is first divided into small square sub-faults. The ground accelerations at a given site ($\ddot{U}_m(t)$), at time t, during the main event, can be synthesized by summing the records of the small events with correction factors as

$$\ddot{U}_m(t) = \sum_{i=1}^{N} C_i \left(\frac{R_0}{R_i} \right) [\ddot{u}_s(t - t_{si} - t_{ri})]. \tag{1}$$

Here $\ddot{u}_s(t)$ is the recorded acceleration for the small event (EGF); C_i the ratio of the stress drop in the ith sub-fault to that of the small event, R_0 the distance between the hypocentre of the small event and the station and R_i is the distance between the ith sub-fault to the station. For each sub-fault, EGF is delayed by the sum of the times t_{si} and t_{ri}. Here, t_{si} is the S-wave travel time from each sub-fault to the station and t_{ri} is the rupture time from the hypocentre to the centre of the sub-fault.

Here, the stress drop ratio (C_i) is estimated from slip distribution as follows[13]

$$C_i = \left[\frac{(A_m / A_s)}{\sum_{i=1}^{N} (d_i / d_{max})^2} \right]^{1/2} \frac{d_i}{d_{max}}, \tag{2}$$

where d_i is the slip on the ith sub-fault and d_{max} is the maximum slip.

As mentioned, the rupture plane of the main shock, which is divided into square shaped sub-faults of area (A_s) is given as

$$A_s = \left[\frac{M_s}{M_m} \right]^{1/2} A_m. \tag{3}$$

Here M_s and M_m are the seismic moments of the small and main events respectively, A_m represents the fault rupture area of the main event.

The source-time function in frequency domain, $S(\omega)$ is of the form[6]

$$S(\omega) = \left(\frac{M_{\mathrm{m}}}{\sum\limits_{i=1}^{N} C_i M_{\mathrm{s}}} \right) \left[\frac{1 + (\omega / \omega_{\mathrm{s}})^2}{1 + (\omega / \omega_{\mathrm{m}})^2} \right], \tag{4}$$

where ω_{s} and ω_{m} are the corner frequencies (in radians) of the small and main events respectively.

The corner frequency for each small event (Hz) is estimated from their seismic moment and stress drop as

$$f_{\mathrm{s}} = 4.9 \times 10^6 V_{\mathrm{s}} \left(\frac{\Delta \sigma}{M_{\mathrm{s}}} \right)^{1/3}, \tag{5}$$

where $\Delta \sigma$ is the stress drop of the small event and V_{s} represents shear-wave velocity of the bedrock near the source region.

For the EGF method, V_{s} is taken as 3.6 km/sec, and $\Delta \sigma$ of small events estimated from the recorded data of a particular event.

Also, the corner frequency of the main event (ω_{m}, radians) is computed as

$$\omega_{\mathrm{m}} = \frac{\omega_{\mathrm{s}}}{\sqrt{M_{\mathrm{m}} / \sum\limits_{i=1}^{N} C_i M_{\mathrm{s}}}}. \tag{6}$$

It can be observed from the above equations, that once the small event corner frequency is known, the source-time function of the main event can be estimated from eq. (4). If information on slip distribution and rutpure velocity (V_r) is available, then the acceleration time history at any station can be obtained with small event recordings at that station using eq. (1), from which the estimated acceleration time histories need to be convolved with the source time function, $S(\omega)$ in eq. (4). For this, the accelerations obtained from the eq. (1) are transformed into frequency domain using fast Fourier transformation (FFT), and convoluted with $S(\omega)$. The final accelerations are obtained by transforming back by inverse fast Fourier transformation (IFFT).

Ground motion estimation for the Coimbatore event (M_w 6) with EGF method

The EGF method, as described in the previous section, is used to simulate ground motion for the 7 February 1900 Coimbatore earthquake (main earthquake), from the available broadband ground motion data for three small events (EGF) occurring in SPI. Figure 2 shows as a sample, the recorded acceleration time histories of the third EGF ($M_{\mathrm{L}} = 3.0$) at 17 stations in the study region. The source details of the main earthquake are taken from

Bhattacharya and Dattatrayam[12]. The moment magnitude for this event is taken as 6 with its epicentre located at 10.7°N and 76.7°E. The strike, dip and focal depth of the rupture plane are taken as 309°, 56° and 9 km respectively. The seismic moment is estimated from magnitude as given in Hanks and Kanamori[14]. The source scaling laws of Mai and Beroza[15] are used to estimate the dimensions of the rupture plane for the main event. The rupture length and width for M_{w} 6 event are obtained as 13 and 8 km respectively. After estimating the rupture dimensions, slip distribution of the main event has to be estimated to obtain stress drop ratio in eq. (2). Since the slip distribution for the main event is not known, it is considered as an anisotropic von Karman random field. The correlation lengths of the slip along the fault dimensions are computed from magnitude using scaling relations reported by Mai and Beroza[15]. To cover all possible slip distributions, 50 samples of Hurst exponent ($h = 0.76 \pm 0.13$) and correlation lengths ($a_x = 6.14 \pm 2.1$ km and $a_y = 2.34 \pm 1.04$ km) are generated using the scaling relations. Once these a_x, a_y and h are known, spectral representation method of Shinozuka and Deodatis[16] is used to simulate 50 samples of slip distributions of the main event. The slip values are tapered at the edges to account for zero slip at the fault edges. Figure 3 shows four samples of slip distribution on the rupture plane. The maximum slip value varies from 95 to 125 cm. Since the slip is random, an ensemble of accelerations time histories is simulated at a given recording station from eq. (1). The shear wave travel time (t_{si}) in eq. (1), for each sub-fault is estimated from the regional velocity model (Table 3)[3]. In the present study, rupture velocity (V_{r}) is taken as 0.8 times the shear wave velocity of the bedrock to estimate the time of rupture (t_{ri}) for each sub-fault. The stress drop ratio (C_i) in eq. (2) is estimated from the slip distributions shown in Figure 3. It can be observed from eq. (4) that the source-time function in frequency domain, $S(\omega)$ depends on the corner frequency of the small event. The corner frequency of the small events (f_{s}) is computed using eq. (5), where the stress drop values for small events are estimated through the method described by Raghukanth and Kavitha[7]. In this method, stress drop value is calculated by mean square error minimization between the horizontal response spectra obtained from recorded data and a stochastic finite fault model[17], called the seismological model. Details about methodology and input parameters of stochastic finite fault model are discussed in the next section. The obtained stress drop values for the three small events are 130, 132 and 140 bars respectively.

For every EGF and station, a total of 50 three-component acceleration time histories are simulated from eq. (1). Since ground motion data from the three small events are available for proper analysis, a total of 150 acceleration time histories are simulated at all the 17 recording stations. Figure 4 shows one sample of simulated
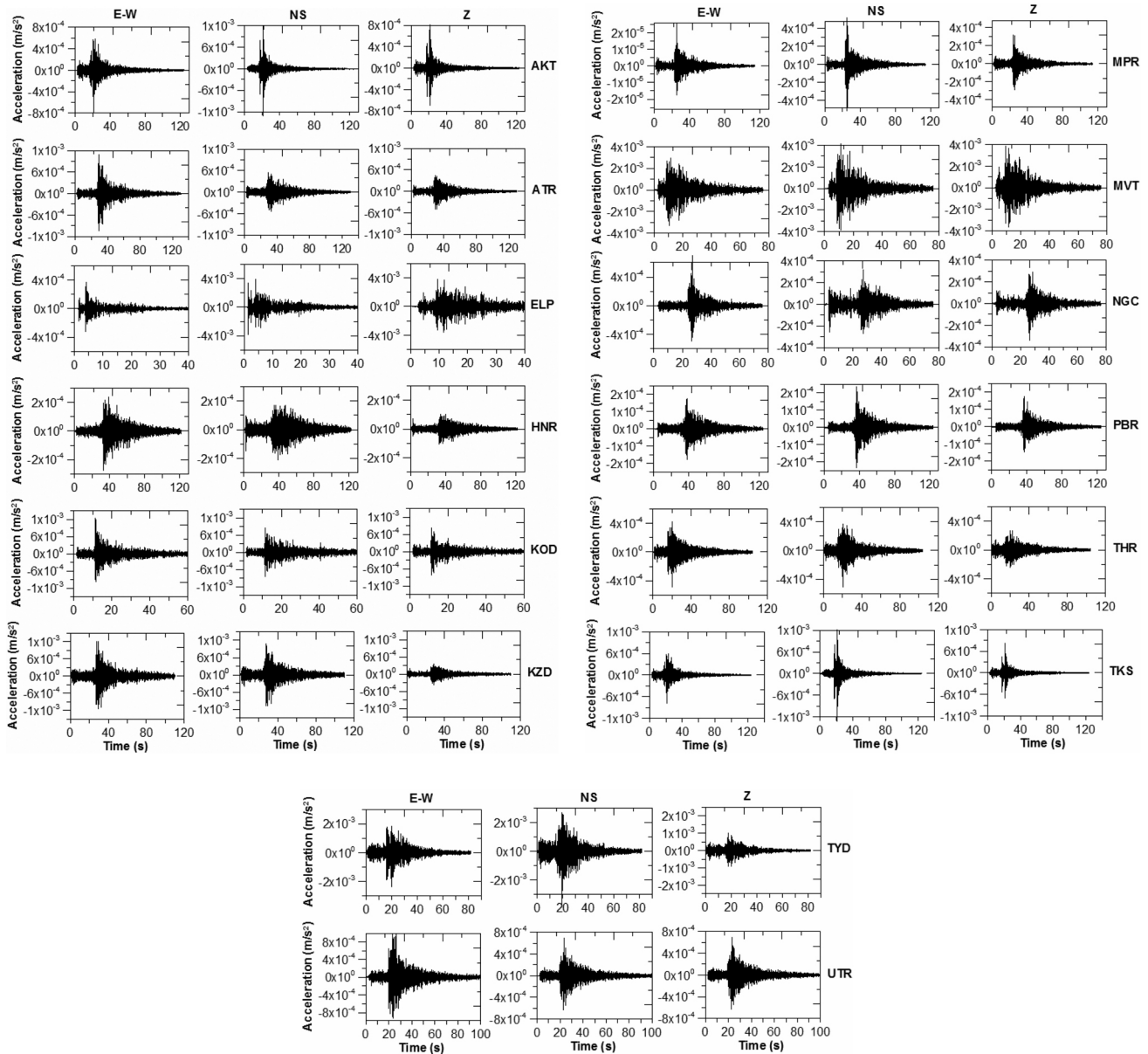
Figure 2. Recorded acceleration time histories of the third EGF (M_L = 3.0) at different stations in the study region.

accelerations for the 1900 Coimbatore event. Response spectra are constructed from the simulated accelerations and mean response is estimated for all stations. Figure 5 shows the estimated mean response spectra at all stations. The minimum and maximum PGAs are estimated from the simulated data (Table 4). It can be noted that the maximum PGA of 0.025 g is obtained at THR (Tharur) station, which is at a distance of 31 km from the epicentre.

Stochastic finite fault model or seismological model

It can be observed from Figure 1 that the average distance between the small events and main event epicentre is

around 100 km, which is a limitation due to the available limited dataset. However, it can be noted that the small (EGF) earthquakes and main event are part of the stable Southern Granulite Terrain (SGT) and contain similar path characteristics. To demonstrate that the path effects are the same between the small (EGF) earthquakes, stations and the main event, and to assess the reliability of the results from the EGF method, ground motions are also estimated using stochastic finite fault model[16]. This model includes the source, path and site effects to simulate the ground motions. In the present study response spectra are also estimated from seismological model and compared with EGF results to verify the consistency of the results.
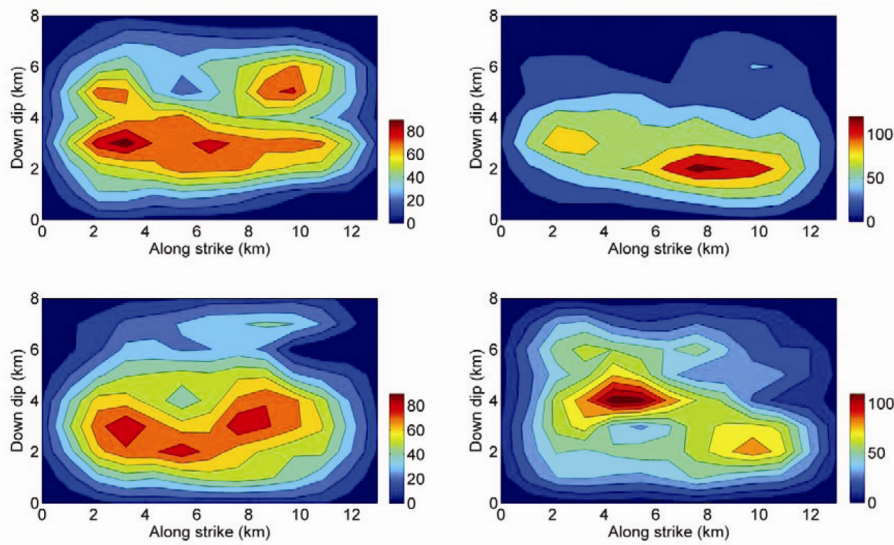
Figure 3. Four sample slip distributions on rupture plan (cm) following the method of Shinozuka and Deodatis[16].

Table 3. Reference regional velocity model

Thickness (km)	V_s (km/sec)	Density (g/cm^3)
1	2.00	2.10
4.0	2.20	2.40
5.0	3.10	2.50
4.0	3.20	2.90
∞	3.60	3.30

Table 4. Estimated horizontal peak ground acceleration (PGA) mean and standard deviation values

Station	PGA (g)
THR	0.025 ± 0.005
MVT	0.018 ± 0.004
KZD	0.024 ± 0.005
ELP	0.006 ± 0.002
HNR	0.008 ± 0.002
AKT	0.009 ± 0.002
TYD	0.012 ± 0.002
SUL	0.002 ± 0.0005
NGC	0.004 ± 0.0008
UTR	0.017 ± 0.004
KOD	0.015 ± 0.002
ATR	0.014 ± 0.003
MTD	0.02 ± 0.005
MPR	0.006 ± 0.002
TKS	0.005 ± 0.001
PBR	0.006 ± 0.001
NLR	0.001 ± 0.0003

In the seismological model, the rectangular fault plane is divided into a number of sub-faults and each sub-fault is represented as a point source. Details are available in the literature[13,17,18]. The Fourier amplitude spectrum (FAS) of ground motion $[Y_j(r, f)]$ due to the jth sub-fault at a site can be expressed as

$$Y_j(r,f) = \frac{\langle R_{\theta\varphi}\rangle\sqrt{2}}{\rho V_s^3} G e^{\left[\frac{-\pi fr}{V_s Q(f)}\right]} \frac{\pi f^2 M_{0j}}{\frac{1}{\sqrt{N}} + \frac{1}{H_j}(f/f_{0j})^2} e^{-\pi\kappa f}.$$

(7)

Here the term involving $\langle R_{\theta\varphi}\rangle\sqrt{2}/\rho V_s^3$ represents a constant multiplying factor, $\langle R_{\theta\varphi}\rangle$ is the radiation coefficient averaged over an appropriate range of azimuths and take-off angles, the coefficient $\sqrt{2}$ represents the product of free surface amplification and partitioning of energy in orthogonal directions; ρ is the density of the medium at focal depth and V_s is the shear velocity in the source region. The term $G e^{[-\pi fr/V_s Q(f)]}$ represents the spatial spread factor. The spatial variation of the ground motion depends on the geometric spreading factor (G), attenuation expressed in the exponential function depends on hypocentral distance (r) and frequency-dependent quality factor $Q(f)$ of the local region. Similarly, the term

$$\frac{\pi f^2 M_{0j}}{\frac{1}{\sqrt{N}} + \frac{1}{H_j}(f/f_{0j})^2} e^{-\pi\kappa f}$$

in eq. (7) represents the contribution of the site-dependent functions, along with kappa factor (κ), the ω^2 source spectral function as a single-frequency model following Aki[19] and Brune[20], and modified Frankel's filter function[16], that account for the observation that the acceleration spectra show sharp decrease with increasing frequency. Here N is the number of sub-faults; f_{0j} the
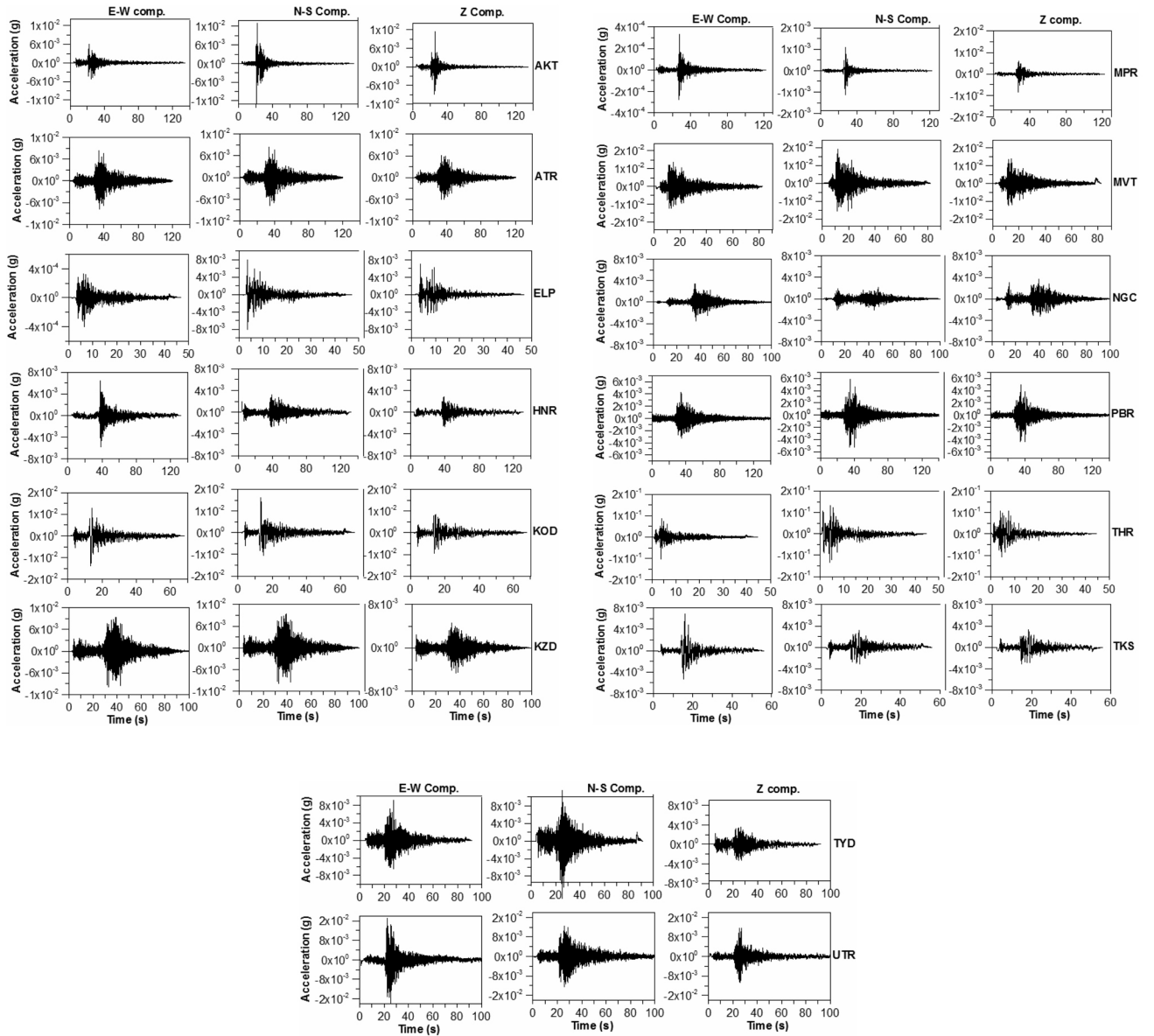
Figure 4. Simulated ground motions from the third EGF event, $M_L = 3.0$.

dynamic corner frequency of the jth sub-fault[21]; H_j the modified scaling factor of the jth sub-fault, which accounts for the observation that the total radiated energy is not conserved with the increase in sub-fault number and M_{0j} is the moment of the jth sub-fault.

In this article, M_{0j} of each sub-fault is calculated from the slip distribution of the fault plane as

$$M_{0j} = \frac{M_0 D_i}{\sum\limits_{j=1}^{N} D_j},\qquad(8)$$

where M_0 is the seismic moment of the event and D_j is the final slip acting on the jth sub-fault. The dynamic corner frequency (f_{0j})[21] is related to the seismic moment and stress drop, and computed as given by

$$f_{0j} = 4.9 \times 10^6 (N_{Rj})^{-1/3} V_s \left(\frac{\Delta\sigma}{M_0 / N}\right)^{1/3},\qquad(9)$$

where V_s is the shear wave velocity in the source region (km/s) at bedrock level, M_0 the seismic moment (dyne-cm), $\Delta\sigma$ the stress drop (bars) giving f_{0j} (Hz) and N_{Rj} is the number of sub-faults ruptured by the time the jth sub-fault is totally ruptured. It can be noted here that f_{0j} goes to f_0 when the whole fault plane is ruptured, and this can be estimated by substituting $N_{Rj} = N$ in eq. (9).
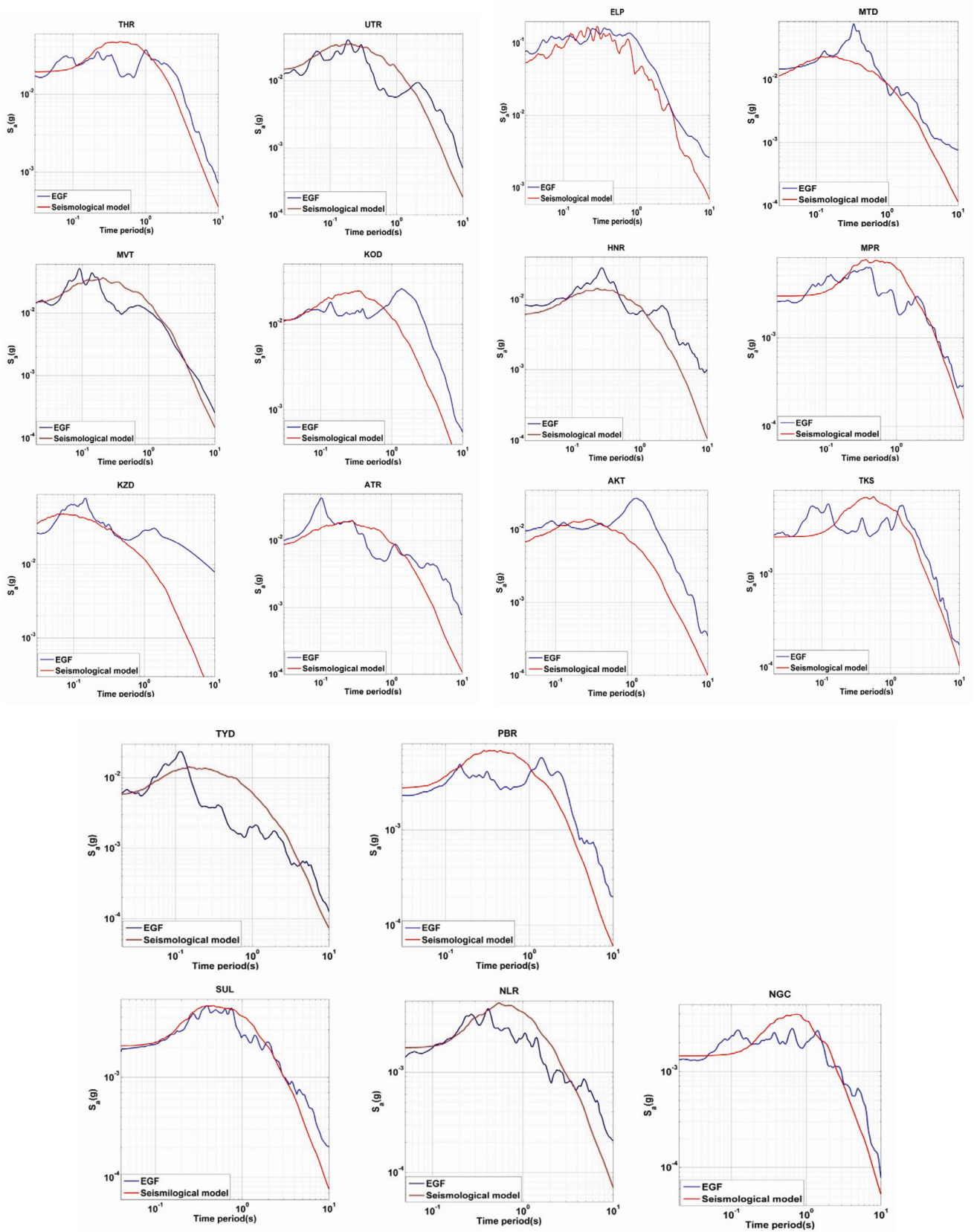
Figure 5. Estimated mean horizontal response spectra for the stations considered in the present study obtained from the EGF method and the seismological model.
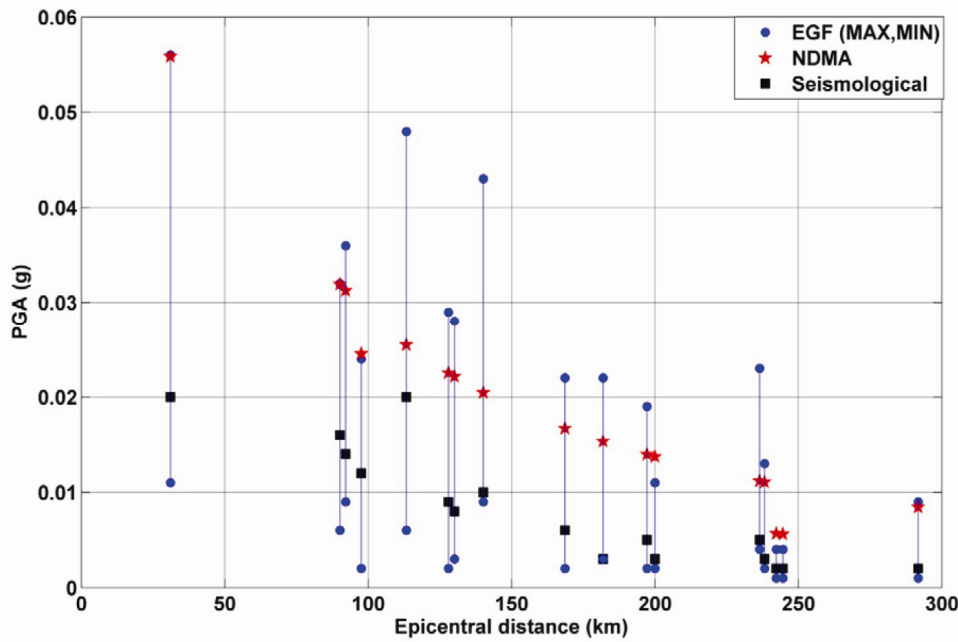
Figure 6. Comparison of estimated Peak Ground Acceleration values using the EGF method, seismological model, and the Ground Motion Prediction Equation given in the National Disaster Management Authority report[8].

The modified scaling factor H_j as per Atkinson and Boore[22] is

$$H_j = \left(N \frac{\Sigma_f \left(\frac{f^2}{1+(f/f_0)^2} \right)^2}{\Sigma_f \left(\frac{f^2}{1+(f/f_{0j})^2} \right)^2} \right)^{1/2}, \tag{10}$$

where f_0 is the corner frequency of the event when the total fault plane is ruptured[20]. Here the dynamic corner frequency (f_{0j}) of the jth sub-fault can be estimated from eq. (9). Motazedian and Atkinson[21] also initiated the idea of pulsing area to additionally account for earthquake rupture. Here the total number of active sub-faults (N_{Rj}) starts at zero at the beginning of rupture and increases as the rupture propagates. However, after the total rupture area reaches a certain value, the number of active sub-faults (N_{Rj}) remains constant, where the parameter (N_{Rj}) represents the number of active sub-faults during rupturing of the jth sub-fault.

It can be noted here that the input parameters like frequency-dependent seismic quality factor $Q(f)$, focal depth, orientation of fault plane, geometric attenuation, and stress drop ($\Delta\sigma$) are region-specific. Here, the seismic quality factor (coda quality factor) developed by Ramakrishna Rao *et al.* (unpublished) for the peninsular India region, $460f^{0.83}$ is used. The general geometrical attenuation term G reported by Singh *et al.*[23] as given in eq. (11) below is used in the present study

$$G = \begin{cases} \dfrac{1}{r}, & \text{for } r \leq 100 \text{ km}, \\[2mm] \dfrac{1}{10\sqrt{r}}, & \text{for } r > 100 \text{ km}. \end{cases} \tag{11}$$

For the present study, the average S-wave radiation coefficient $\langle R_{\theta\varphi} \rangle$ of 0.55 is considered[24]. Atkinson and Boore[22] reported that the pulsing percentage has limited sensitivity on accelerations. In the present study, an average value of 50%, i.e. between 25% and 75% is used to simulate ground motions. Here stress drop ($\Delta\sigma$) and kappa (κ) are considered as random variables. Singh *et al.*[23] reported the stress drop value range from 100 to 300 bar for events in Peninsular India. Chandler *et al.*[25] developed an empirical equation to estimate the kappa value from the average shear wave velocity of the top 30 m (V_{s30}) as

$$\kappa = \frac{0.057}{V_{s30}^{0.8}} - 0.02. \tag{12}$$

For a given station, based on the local site condition, the range of kappa value is estimated from eq. (12). The estimated κ range for the station ATR, which belongs to B-type site (760 m/s < V_{s30} < 1500 m/s), is 0.02–0.05. The Latin Hypercube sampling technique developed by Iman and Conover[26] is used generate a total of 50 random combinations of stress drop and kappa. From the description stochastic finite fault approach, it can be seen that once the region and site parameters are known, FAS of

ground acceleration can be simulated for a given magnitude (M_w) and hypocentral distance (r).

Computationally, the seismological method described above involves three steps in retrieving the accelerograms from eq. (7). First, the strong motion corresponding to each sub-fault is assumed as a Gaussian white noise having a sample length equal to the strong motion duration

$$T = (1/f_{0j} + 0.05r_j), \qquad (13)$$

where f_{0j} is the dynamic corner frequency of the sub-fault and r_j is the distance from the centre of the jth sub-fault to the station. This white noise sample is then multiplied by a non-stationary modulating function. The modulating function suggested by Saragoni and Hart[27] is used in the present study. Next the sample is transformed into frequency domain using Fourier transformation. Further, this spectrum is normalized by the root mean-square value and multiplied by eq. (7). The ground motion for each sub-fault can be obtained by transforming the resulting spectra from frequency domain to time domain. The simulated accelerations from all sub-faults are summed up with proper time delay Δt_j, which accounts for the rupture velocity to obtain the final acceleration of a given magnitude earthquake

$$a(t) = \sum_{j=1}^{N} a_j(t + \Delta t_j). \qquad (14)$$

For a given station, the mean response spectrum is estimated from the 50 samples of simulated acceleration time histories. Figure 5 provides a comparison of mean horizontal response spectra obtained from the EGF method and the seismological model for all 17 stations. It can be observed that the simulated response spectra from both the approaches are in agreement with each other. The response spectra obtained from the EGF method and the seismological model are reasonably comparable, with some minor variations, possibly due to the local soil conditions.

Ground motion prediction equations

The ground motion prediction equations (GMPE) widely used in Peninsular India can be used for comparison with the present estimated results. Raghukanth and Iyengar[3] developed GMPE for Peninsular India based on stochastic seismological model of Boore[17]. This prediction equation is updated in the NDMA report[8]. The GMPE for Peninsular India region can be written as

$$\ln(PGA(g)) = -5.22 + 1.65M - 0.03M^2 - 0.003r$$
$$- 1.44 \ln(r + 0.02e^{0.99M}) + 0.12 \log(r)f_0, \qquad (15)$$

where

$$f_0 = \max(\ln(r/100), 0), \quad \sigma(\varepsilon) = 0.38. \qquad (16)$$

Here, M and r represent the moment magnitude and hypocentral distance (km) respectively. The PGA values obtained from the above GMPE are valid for A-type site condition where shear wave velocity in the top 30 m is higher than 1.5 km/s (ref. 28). Table 4 lists the PGAs at all the 17 stations in this study, obtained from the above eq. (15). Since A-type rocks are commonly encountered in SPI, eq. (15) can be used to validate the PGA values obtained from the EGF technique. Figure 6 provides a comparison between the PGA values obtained from GMPE, EGF and seismological models. It can be observed that out of 17 stations, at 14 stations the PGAs obtained from eq. (15) lie in the bounds obtained from EGF. The mean PGA values are also within the bounds of the maximum and minimum PGA values obtained from the EGF method. The differences at some stations can be attributed to the local site conditions.

In the literature, empirical equations are available to estimate PGA values from modified Mercalli intensity (MMI) values. Hough and Bilham[29] reported MMI values for the 1900 Coimbatore earthquake at 38 different stations. In the present study, out of 38 stations, ground motions are simulated at only 2 stations (KOD, KZD), and the reported MMI values at these 2 stations are V and IV respectively. Iyengar and Raghukanth[2] reported an empirical equation between PGA and MMI for Indian conditions; it can be expressed as

$$\ln(PGA)/g = 0.6782\ MMI - 6.8163; \quad \sigma \ln(\varepsilon) = 0.7311. \qquad (17)$$

The estimated PGA values at stations KOD and KZD from eq. (17), are 0.032 and 0.016 g respectively. The corresponding mean PGA values obtained from the EGF method are 0.015 and 0.02 g respectively, which shows the fairly comparable PGA values at these two stations.

Summary and conclusion

Acceleration time history is the most significant information required for engineering purposes during a damaging event. It is required to study and understand the behaviour of structures during an earthquake and to predict future hazards in a region. This article estimates possible ground motion for an M_w 6 event in southern India using EGF methodology. Here, the small events lying near the focal region of the main, i.e. 1900 Coimbatore event, are treated as EGFs, using model corrections. The fault location and orientation for the main shock are taken as reported for the 1900 Coimbatore event. The rupture dimensions are fixed from source scaling relations based on magnitude of the main shock. The slip distribution is simulated as a random field. The stress drop of the three

small events estimated from stochastic seismological model lies between 130 and 140 bar. An ensemble of accelerations and response spectra is simulated at all these 17 stations using the corresponding EGFs. Stochastic seismological model is also used to simulate the ground motion of the Coimbatore event. The input parameters like stress drop ($\Delta\sigma$) and kappa (κ) are considered as random variables to simulate the ground motions. The mean response spectra are estimated from simulated ground motions and compared with EGF results. The good similarity of results shows that the obtained results from the EGF and the seismological model are consistent with each other. The obtained PGAs are consistent with those obtained from GMPE of NDMA report[8], widely used in Peninsular India. We observed that maximum PGA of 0.025 g is obtained at station THR, which is at a distance of 31 km from the epicentre. Although the obtained results are valid for the 1900 Coimbatore earthquake, the simulated acceleration time histories can be used to understand the seismic response of structures like man-made constructions such as bridges and dams, and other structures, for any event of magnitude M_w 6 in SPI.

1. Rajendran, C. P., John, B., SreeKumari, K and Rajendran, K., Re-assessing the earthquake hazard in Kerala based on the historical and current seismicity. *J. Geol. Soc. India*, 2009, **73**, 785–802.
2. Iyengar, R. N. and Raghukanth, S. T. G., Attenuation of strong ground motion in Peninsular India. *Seismol. Res. Lett.*, 2004, **75**(4), 530–540.
3. Raghukanth, S. T. G. and Iyengar, R. N., Estimation of seismic spectral acceleration in Peninsular India. *J. Earth Syst. Sci.*, 2007, **116**(3), 199–214.
4. IS 1893, Criteria for earthquake resistant design of structures. Bureau of Indian Standards, Part 1, General Provisions and Buildings, 2002.
5. Hartzell, S. H., Earthquake aftershocks as Green's functions. *Geophys. Res. Lett.*, 1978, **5**, 1–4.
6. Frankel, A., Simulating strong motion of large earthquakes using recordings of small earthquakes: the Loma Prieta mainshock as test case. *Bull. Seismol. Soc. Am.*, 1995, **85**, 1144–1160.
7. Raghukanth, S. T. G. and Kavitha, B., Stochastic finite fault modeling of subduction zone earthquakes in northeastern India. *Pure Appl. Geophys.*, 2013, **170**, 1705–1727.
8. NDMA Report, Development of probabilistic seismic hazard map of India. Final Technical Report of the Working Committee of Experts, constituted by the National Disaster Management Authority, Government of India, 2010.
9. Rai, S. S. *et al.*, The South India Precambrian crust and shallow lithospheric mantle: Initial results from the India Deep Earth Imaging Experiment (INDEX). *J. Earth Syst. Sci.*, 2013, **122**(6), 1435–1453.
10. Rajendran, K. P., Talwani, P. and Gupta, H. K., State of stress in the Indian subcontinent: a review. *Curr. Sci.*, 1992, **62**, 86–93.
11. Saikia, U., Rai, S. S., Subrahmanyam, M., Dutta, S., Bose, S., Borah, K. and Meena, R., Accurate location and focal mechanism of small earthquakes near Idukki Reservoir, Kerala: implication for earthquake genesis. *Curr. Sci.*, 2014, **107**, 1884–1891.
12. Bhattacharya, S. N. and Dattatrayam, R. S., Earthquake sequence in Kerala during December 2000 and January 2001. *Curr. Sci.*, 2002, **82**, 1275–1278.
13. Pitarka, A., Somerville, P., Fukushima, Y., Uetake, T. and Irikura, K., Simulation of near-fault strong-ground motion using hybrid Green's functions. *Bull. Seismol. Soc. Am.*, 2000, **90**, 566–586.
14. Hanks, T. C. and Kanamori, H., A moment magnitude scale. *J. Geo-Phys. Res.*, 1979, **84**, 2348–2350.
15. Mai, P. M. and Beroza, G. C., A spatial random field model to characterize complexity in earthquake slip. *J. Geophys. Res.*, 2002; doi:10.1029/2001JB000588.
16. Shinozuka, M. and Deodatis, G., Simulation of multi-dimensional Gaussian stochastic fields by spectral representation. *Appl. Mech. Rev.*, 1996, **49**(1), 29–53.
17. Boore, D. M., Comparing stochastic point-source and finite-source ground-motion simulations: SMSIM and EXSIM. *Bull. Seismol. Soc. Am.*, 2009, **99**, 3202–3216.
18. Boore, Simulation of ground motion using the stochastic method. *Pure Appl. Geophys.*, 2003, **160**, 635–676.
19. Aki, K., Scaling law of seismic spectrum. *J. Geophys. Res.*, 1967, **72**, 1217–1231.
20. Brune, J. N., Tectonic stress and the spectra of seismic shear waves from earthquakes. *J. Geophys. Res.*, 1970, **75**, 4997–5009.
21. Motazedian, D. and Atkinson, G. M., Stochastic finite-fault modeling based on a dynamic corner frequency. *Bull. Seismol. Soc. Am.*, 2005, **95**, 995–1010.
22. Atkinson, G. M. and Boore, D. M., Earthquake ground-motion prediction equations for eastern North America. *Bull. Seismol. Soc. Am.*, 2006, **96**, 2181–2205.
23. Singh, S. K., Garcia, D., Pacheco, J. F., Valenzuela, R., Bansal, B. K. and Dattatrayam, R. S., Q of the Indian Shield. *Bull. Seismol. Soc. Am.*, 2004, **94**, 1564–1570.
24. Boore, D. M. and Boatwright, J., Average body-wave radiation coefficients. *Bull. Seismol. Soc. Am.*, 1984, **74**, 1615–1621.
25. Chandler, A. M., Lam, N. T. K. and Tsang, H. H., Near-surface attenuation modelling based on rock shear-wave velocity profile. *Soil Dyn. Earth Eng.*, 2006, **26**, 1004–1014.
26. Iman, R. C. and Conover, W. J., Small sample sensitivity analysis techniques for computer models with an application to risk assessment. *Commun. Stat. Theory Methods*, 1980, **A9**(17), 1749–1842.
27. Saragoni, G. R. and Hart, G. C., Simulation of artificial earthquakes. *Earthquake Eng. Struct. Dyn. J.*, 1974, **2**, 249–268.
28. IBC, International Building Code, International Code Council (ICC), 2009.
29. Hough, S. E. and Bilham, R., Site response of the Ganges Basin inferred from re-evaluated macroseismic observations from the 1897 Shillong 1905 Kangra and 1934 Nepal earthquakes. *J. Earth Syst. Sci.*, 2008, **117**, 773–782.